Methods for measuring the masses of stellar black holes and neutron stars

Samppa Alatalo
B.Sc. thesis
Degree Programme in Physics
Faculty of Science
University of Oulu
September 2021

Contents

1 Introduction

Stellar black holes and neutron stars are remnants of massive stars that have burned through their fuel supply, resulting in their collapse. The mass of the remnant left over after its outer layers are gone determines the type of compact star it forms. The lightest ones form white dwarfs, then neutron stars and the most massive remnants collapse into black holes.

Neutron stars are extremely dense stars held together by neutron degeneracy pressure and strong force repulsion. Their radii are only on the order of 10 km with masses in the 1–2 $M_\odot$ range. This results in densities on the order of $10^{17}\,\mathrm{kg/m^3}$. Most neutron stars are observed as pulsars, meaning that they emit beams of electromagnetic radiation from their magnetic poles. Neutron stars have very short rotational periods and their magnetic poles are not necessarily aligned with their rotational axes, so the beams of radiation coming from pulsars are seen as periodic pulsations. Other types of neutron stars include magnetars, which have magnetic fields about a thousand times stronger than normal, and combinations of pulsars and magnetars.

Black holes are extreme objects where the entirety of their mass is condensed into a single point in space; a singularity. Stellar black holes are formed when a collapsing star is so massive that nothing can stop the collapse of its core. The extreme nature of these objects creates some unique characteristics. For example, the black hole itself can never be seen. Rather, the only theoretically visible part is the event horizon, which is the boundary whereafter the escape velocity exceeds the speed of light. This also means that black holes are only currently detectable by indirect means, most commonly through bursts of radiation created by the accretion of matter in a binary system, as the far less dense companion loses matter as it falls into the black hole. The accretor in these systems can also be a neutron star or a white dwarf. More recently, gravitational waves have been detected from mergers in

binary black hole and neutron star systems, and even black hole and neutron star mergers (see GraceDB for events).

The aforementioned binary systems are the most important subjects of analysis. They are called X-ray binaries, after the X-rays emitted from accretion; the flow of matter between the objects. As mentioned above, these systems contain a compact accretor – a black hole or a neutron star – and a companion star, often referred to as the donor. The mass of the donor star determines whether the system is considered a low- or high-mass X-ray binary, with donor masses upwards of about $10\,M_\odot$ considered high-mass. A more rare intermediate-mass X-ray binary classification is also used for some binaries with around 1–3 $M_\odot$ Roche-lobe filling companions [1]. The strong gravitational pull of the compact object causes gas from the companion star to be stripped away and fall toward the accretor. This gas then forms a disc known as an accretion disc, where the gas heats up through viscosity, causing the emission of X-rays from the inner portion of the accretion flow. Not all matter makes it onto the accretor either; outflows are streams of matter that get launched from different regions of the accretion flow. If the accretor is a neutron star, the accretion process can change its mass significantly in old low-mass X-ray binaries. For black holes, however, the accreted mass is too low to cause significant alteration, and for neutron stars in high-mass X-ray binaries the accretion is either too weak or non-existent on top of the fact that the systems are short-lived [1].

Low-mass X-ray binaries can be transient or persistent, meaning that the X-ray emission can vary or stay relatively consistent. X-ray transients show periodic outbursts, where the X-ray luminosity increases, peaks and then decays back to quiescence. The quiescent phase is typically much longer than an outburst, which commonly lasts between weeks to months. Transient low-mass X-ray binaries usually contain a black hole, while persistent ones con-

tain a neutron star. For details, see [1].

Transient black hole binaries also display different states of accretion. These states and their transitions follow repeating cyclical patterns, which can be visualised on a hardness-intensity diagram (HID), similarly to the Hertzsprung-Russell diagram. Figure 1 depicts a typical HID. The different accretion states affect the intensity of the radiation coming from the source, i.e. its luminosity. Note that the HID does not generally include the quiescent phase, because most X-ray telescopes are not sensitive enough to detect such low luminosity sources. For a recent detailed review on these properties and more, see [2].

The most important factor in distinguishing a black hole from a neutron star (or the compact objects in general) is the object's mass. The maximum mass for white dwarfs is known as the Chandrasekhar limit, about $1.4\,M_\odot$. Compact stars heavier than this and up to about $2.1\,M_\odot$ [3] – also known as the Tolman-Oppenheimer-Volkoff limit – are expected to be neutron stars, but a minimum mass of about $1.1\,M_\odot$ and a maximum of up to $2.6\,M_\odot$ have been brought up [3, 4]. Remnants with masses above this maximum are thought to collapse all the way into a singularity, forming a stellar black hole. The masses of these extreme objects can range from a few up to several tens of solar masses [5]. However, the minimal possible mass found is about $4.3\,M_\odot$ [6], which is far above the maximum neutron star mass.

This mass gap in the $2–5\,M_\odot$ area of the compact object mass distribution has been an active topic of discussion. For example, harsh systematic errors resulting from different states of X-ray variability (see section 2.1) have been shown to cause overestimates of masses [7], while gravitational wave observations have shown some support for the existence of this mass gap [4]. Regardless, the discussion around this subject is ongoing and further analysis is still needed.

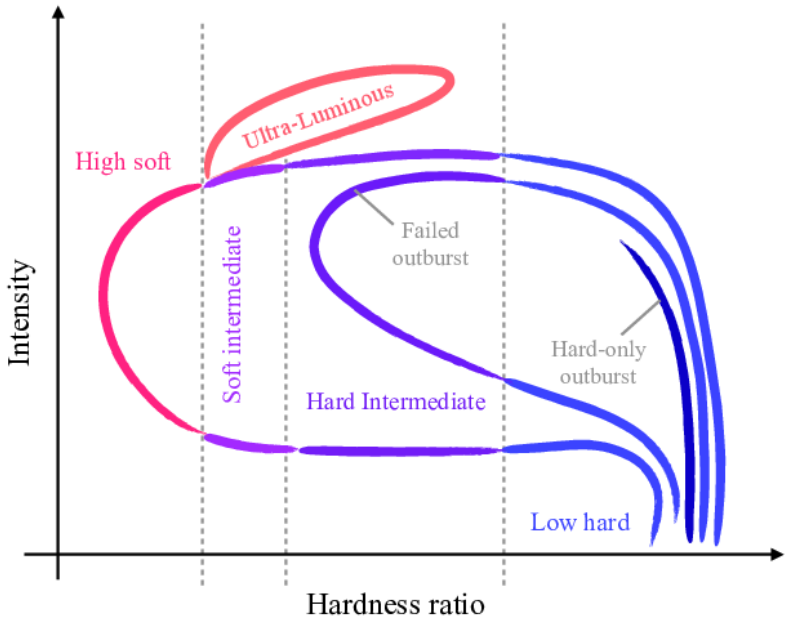

Figure 1. A typical hardness-intensity diagram (HID) showing different accretion states and their transitions. During an outburst, the loop is travelled anti-clockwise, starting from the bottom right corner. From [2]. *Reprinted from* New Astronomy Reviews*, 93, S. E. Motta et al., The INTEGRAL view on black hole X-ray binaries, 101618, 2021, with permission from Elsevier. https://doi.org/10.1016/j.newar.2021.101618.*

Due to the elusive nature of these objects, determining their masses can be challenging and subject to large error margins. Nonetheless, several methods have been developed to help with the task.

2 Methods

In this section, the general properties of the methods used for mass determination are described by dividing them into three broad classes: dynamical, scaling and spectra fitting methods [5]. However, this division is not absolute

and they often overlap and/or blend into one another. In practice, different methods are used in conjunction while looking for consistencies.

2.1 Dynamical methods

Dynamical methods are considered the most common and important methods for measuring the masses of black holes and neutron stars. They are based on the Keplerian motion of a test particle around the object. At their base, the general idea is simple: for a test particle on a circular orbit around the body, if we can measure its velocity v and the radius of the orbit R, we can obtain the object's mass as [5]

$$M = \frac{Rv^2}{G}. \tag{1}$$

This basic idea is then complicated by several real-world factors depending on the test particle selection. The inclination of the orbit is the biggest challenge as the measurement of just one of the particle's velocity components is not enough for determining the orbital speed [5].

For our context of stellar black holes and neutron stars, the dynamical method requires an X-ray binary system. These are commonly found as X-ray transients [8]. An X-ray transient in its quiescent state can allow for the optical or near-infrared detection of the donor star, if the X-ray emission is not strong enough to mask it. However, many complications can make this task difficult. The donor star is often small, namely in short period X-ray binaries. Additionally, these systems tend to be quite far away, which means that the companion can be very faint. This difficulty in detection is evident in our relatively low number of dynamically confirmed black holes. But, if the conditions allow, the donor's light curve and spectrum can be observed, which reveals a lot about the system's dynamical properties. The photospheric absorption lines on the donor's spectrum can be compared to a stellar template of a similar spectral type in order to infer its radial velocity curve based on

redshift [8]. However, for accurate radial velocity measurements, the system's inclination angle to us needs to be sufficiently high, i.e. it should be seen almost edge-on. As seen in figure 2, this curve will form a sine wave with possible distortions based on the orbit's ellipticity, although the orbits can be expected to be decently circular in most cases, at least in low-mass X-ray binaries [9]. The peaks of this curve will then provide the peak radial velocity, known therefore as radial velocity semi-amplitude. The curve will additionally provide the period of the orbit.

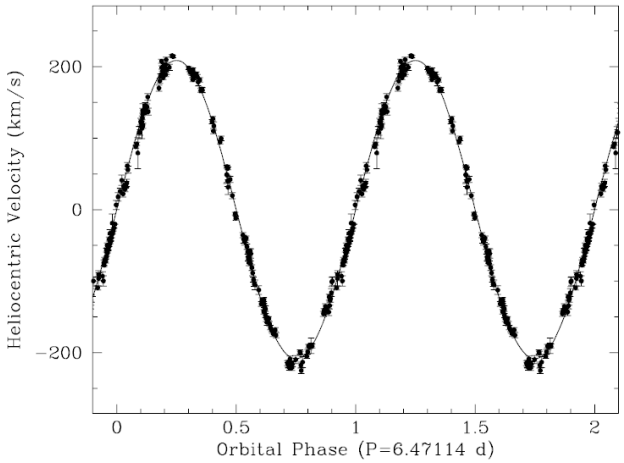

Figure 2. An example radial velocity curve from the K0 donor star in V404 Cyg [8]. *Reprinted by permission from Springer Nature Customer Service Centre GmbH: Springer Nature,* Space Science Reviews*, Mass Measurements of Stellar and Intermediate-Mass Black Holes, J. Casares, P. G. Jonker, 2013.*

The absorption lines can also be used to constrain the mass ratio of the binary. Mass ratio is the ratio between the companion's mass and the compact star's mass. As a result of the donor star filling its Roche lobe and being tidally locked, the lines show significant rotational broadening, which can be compared to a slowly rotating template convolved with a limb-darkened rotational profile [8], like in figure 3. A limb-darkened rotational profile refers

to a model of the star's rotation that takes into account its limb darkening effects, where the star appears brighter toward the centre. The mass ratio can then be constrained, as the rotational broadening scales with the donor's velocity under the approximation of sphericity as [10]

$$V \sin i / K_{\rm c} \simeq 0.462 q^{1/3} (1+q)^{2/3}, \tag{2}$$

where $V \sin i$ is the rotational broadening of the absorption lines, $K_{\rm c}$ is the velocity of the companion star and q is the mass ratio.

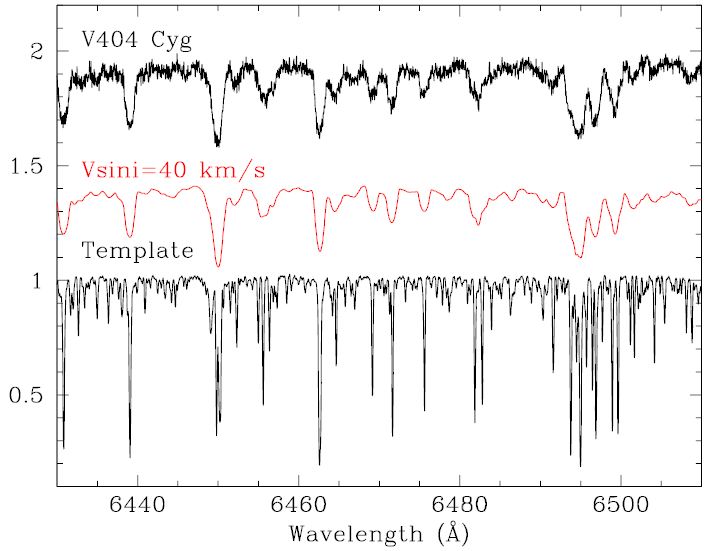

Figure 3. Rotational broadening analysis. There is a template star (bottom), the rotational profile (middle) and the donor star's spectrum (top). The template (a K0IV star) is broadened by $V \sin i = 40\,\mathrm{km/s}$ (rotational profile), which reproduces the spectrum of the donor star located in V404 Cyg [8]. *Reprinted by permission from Springer Nature Customer Service Centre GmbH: Springer Nature,* Space Science Reviews*, Mass Measurements of Stellar and Intermediate-Mass Black Holes, J. Casares, P. G. Jonker, 2013.*

The light curve can be used to obtain the binary inclination by fitting the optical or near-infrared light curves with synthetic ellipsoidal models, as seen in figure 4. The amplitude of the double-humped modulation in the light curves is a strong function of the inclination angle [8].

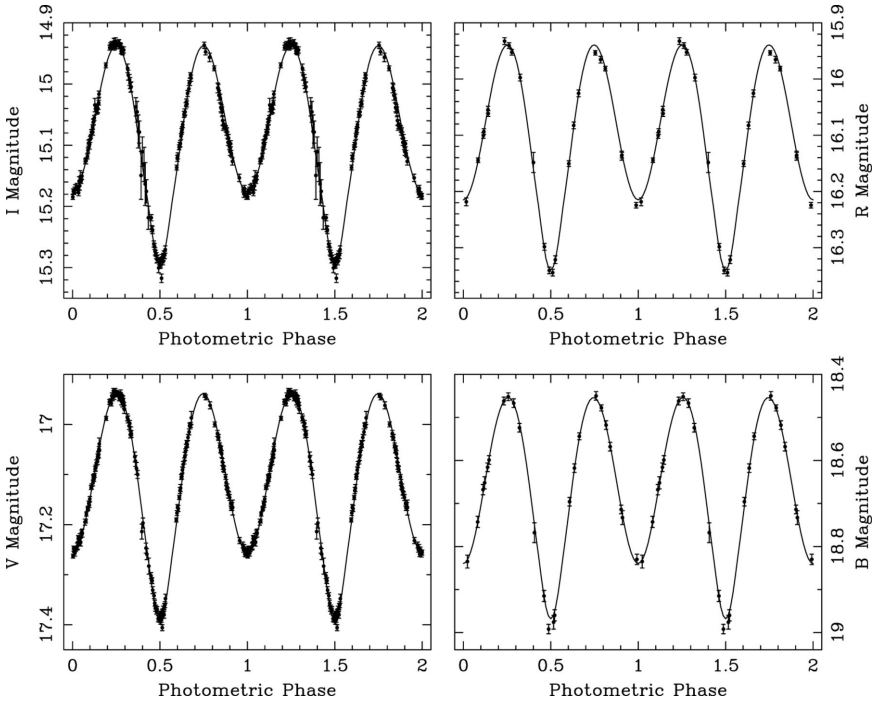

Figure 4. Fitting the light curves of GRO J1655-40 with ellipsoidal models in four colour bands simultaneously [8]. *Source: Figure 2, The quiescent light curve and the evolutionary state of GRO J1655–40, M. E. Beer, P. Podsiadlowski,* Monthly Notices of the Royal Astronomical Society*, Volume 331, Issue 2, March 2002, Pages 351–360, https://doi.org/10.1046/j.1365-8711.2002.05189.x.*

The companion star takes the role of the test particle, but since the companion itself is also non-negligibly massive, we can not directly isolate the compact star's mass. Thus, all the measured information is combined in the binary mass function. Kepler's Third law of motion states that the squares of

the orbital periods of orbiting objects are directly proportional to the cubes of the semi major axes of their orbits $P_{\mathrm{orb}}^2 \propto a^3$. This, in combination with Newton's law of gravitation, provides us with the binary mass function for the mass M_{X} of a compact X-ray source

$$f(M_{\mathrm{X}}) = \frac{K_{\mathrm{c}}^3 P_{\mathrm{orb}}}{2\pi G}\left(1-e^2\right)^{\frac{3}{2}} = \frac{M_{\mathrm{X}}^3 \sin^3 i}{(M_{\mathrm{X}}+M_{\mathrm{c}})^2} = \frac{M_{\mathrm{X}} \sin^3 i}{(1+q)^2} \tag{3}$$

and, alternatively, for the mass M_{c} of the companion star

$$f(M_{\mathrm{c}}) = \frac{K_{\mathrm{X}}^3 P_{\mathrm{orb}}}{2\pi G}\left(1-e^2\right)^{\frac{3}{2}} = \frac{M_{\mathrm{c}}^3 \sin^3 i}{(M_{\mathrm{X}}+M_{\mathrm{c}})^2} = \frac{M_{\mathrm{c}} \sin^3 i}{(1+q^{-1})^2}, \tag{4}$$

where K_{c} and K_{X} are the respective radial velocity semi-amplitudes, e is the eccentricity of the orbit, i is inclination, $q = M_{\mathrm{c}}/M_{\mathrm{X}} = K_{\mathrm{X}}/K_{\mathrm{c}}$ is the mass ratio of the binary and G is the gravitational constant. As mentioned previously, for low-mass X-ray binaries, the eccentricity is expected to be fairly circular in most systems, which means that $e = 0$, giving $\left(1-e^2\right)^{3/2} = 1$, simplifying the function further.

The mass function (3) can be used to infer a lower limit for the object's mass by setting $M_{\mathrm{c}} = 0$ and $i = \frac{1}{2}\pi = 90°$ (edge-on geometry). In order to get a more specific value, one would need an estimate of the inclination of the orbit i and another for the mass of the donor star M_{c}. These values can be more or less constrained for example by using multiwavelength measurements and applying evolutionary constraints [5].

There are, however, considerable sources of systematic error involved. In (3) and (4), one can see that the mass function is cubically dependent on the inclination angle i. This means that uncertainties in inclination dominate the errors in mass measurements. Inclination in general is challenging to determine, and there are many examples of independent research groups performing ellipsoidal fits on the same binary but resulting in a wide spread of inclinations [8]. Two main sources are recognised for the systematic error causing this in the light curve analysis.

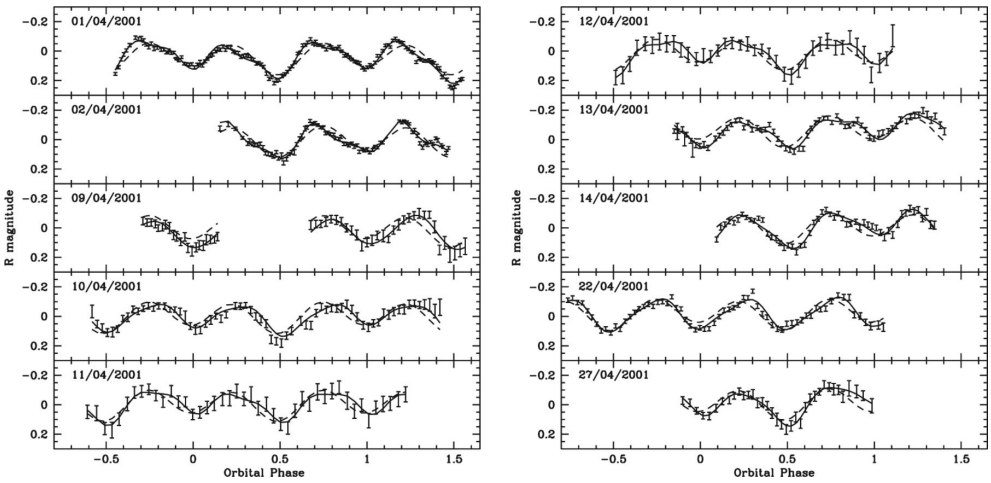

Figure 5. Superhump modulation seen in the ellipsoidal light curves of XTE J1118+480. The continuous line represents a combined model of an ellipsoidal plus superhump waves, providing a better description of the data, while the dashed line represents a pure ellipsoidal fit [8]. *Source: Figure 4, Detection of superhumps in XTE J1118+480 approaching quiescence, C. Zurita et al.,* Monthly Notices of the Royal Astronomical Society*, Volume 333, Issue 4, July 2002, Pages 791—799, https://doi.org/10.1046/j.1365-8711.2002.05450.x.*

The first is the presence of a so-called superhump modulation [8]. It is a distorting wave caused by the accretion disc turning eccentric and precessing with a longer timescale than the orbital period. It appears as a hump in brightness on the light curve, as seen in figure 5. Potential superhump waves can be distinguished from the true ellipsoidal modulation with intensive monitoring over several orbital cycles. Fortunately, the periods of X-ray binaries are relatively short, usually in the scale of weeks or even hours.

The second source is the more mysterious contamination from rapid aperiodic variability [8]. This is seen as fast and erratic flaring in an X-ray transient's light curve in its quiescent state, as illustrated in figure 6. Some of the

variability's properties point toward an accretion disc origin, but ultimately the physical mechanisms responsible remain unknown. However, two main states of variability have been identified: passive and active states [8]. In the passive state, the system becomes redder while displaying minimal flaring activity. Light curves measured outside of the passive state can yield significantly lower inclinations, resulting in overestimated masses. Therefore it is critical to use light curves with minimal flaring activity measured during passive states.

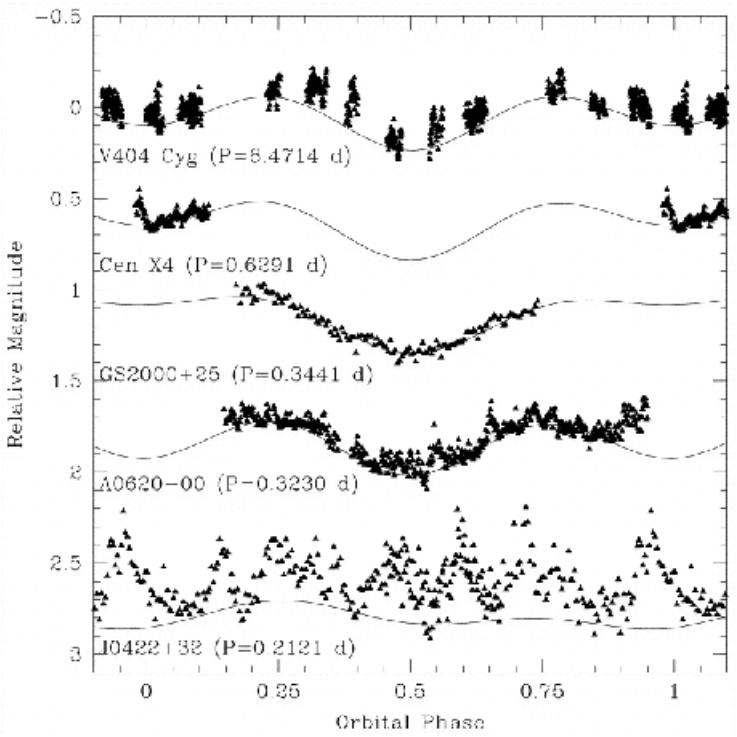

Figure 6. Fast variability as seen in the high-time resolution light curves of five different X-ray transients [8]. *Source: Figure 1, Evidence for Optical Flares in Quiescent Soft X-Ray Transients, C. Zurita, J. Casares, T. Shahbaz,* The Astrophysical Journal, *Volume 582, Issue 1, January 2003, Pages 369–381, https://doi.org/10.1086/344534.*

There are several situational caveats related to these methods. These will be discussed in section 3.

2.1.1 Example case MAXI J1305-704

To illustrate the dynamical method, this example summarises a recent dynamical confirmation of a black hole in MAXI J1305-704 (hereafter referred to as J1305) by Sánchez et al. [11]. By using the Gamma-Ray burst Optical/Near-infrared Detector GROND and the Very Large Telescope Unit Telescope 1 (VLT-UT1), the group managed to observe the optical companion of the binary in quiescence, which had so far proven too faint for analysis. The analysis had to be limited to optical bands due to a nearby field star at a separation of $1.64''$. J1305 has a generally low signal-to-noise ratio in near-infrared wavelengths and the detectors have a coarser pixel size of about $0.60''$/pixel, which means that the near-infrared flux would not be possible to isolate from the nearby star's. In optical wavelengths the potential contamination was deemed negligible, allowing for reliable spectroscopy.

The final spectroscopic dataset consisted of 16 spectra. In low-mass X-ray binaries the accretion disc does not completely disappear during quiescence, which makes the companion star's absorption lines appear shallower or even undetectable. To accommodate this lack of reliable flux calibration, the group performed a low-order polynomial fit on the continuum of spectra and then divided each spectrum by it, thus creating normalised spectra.

In order to derive the radial velocity curve of the companion, the group compared each spectrum with stellar templates. They could then create cross-correlation functions (CCFs) and select the best-fitting template. This let them map out a trail of CCFs and perform a sinusoidal fit on it, as seen in figure 7. They identified a second, stationary peak on the trail, but later attributed it to contamination from the nearby star mentioned earlier.

After their analysis, the group derived the following parameters: radial velocity semi-amplitude of the companion star $K_c = 554 \pm 8\,\mathrm{km/s}$, spectroscopic period[1] of the binary $P_{spec} = 0.394 \pm 0.004\,\mathrm{d}$, systemic radial velocity $\gamma = -9 \pm 5\,\mathrm{km/s}$ (i.e. the radial velocity of the centre of mass of the binary) and $T_0 = 2457479.6705 \pm 0.0013$, the Barycentric Julian Date (BJD) for the zero phase, which corresponds to the companion star inferior conjunction.

Through statistical analysis of the normalised averaged spectrum of J1305 against a modified template spectrum of a K0V star[2], the group managed to extract values for the rotational broadening of the absorption lines $V \sin i < 110\,\mathrm{km/s}$, surface gravity $\log g > 4.42$, effective temperature $T_{\mathrm{eff}} = 4610^{+130}_{-160}\,\mathrm{K}$ and a veiling factor in the r′ band $X = 0.66 \pm 0.04$, which they define as the ratio of fluxes of non-stellar origin (like an accretion disc) to the total emitted light. These are used mainly for spectral classification, apart from the rotational broadening, which is of course also crucial for the mass determination. It was used to get an independent determination of the mass ratio q with (2) as $q < 0.07$.

To model the light curve, the group employed four different models. The details are skipped here, but see the original paper [11], especially to note the sensitivity of the inclination value between the models. The model deemed to be the best fit (called A2 in the original paper) used normalised-flux light curves, included only the g′, r′ and i′ photometry due to their high signal-to-noise data and removed veiling effects in the r′ band during the fit. The model resulted in several parameters, notably the photometric period $P_{\mathrm{phot}} = 0.3958 \pm 0.018\,\mathrm{d}$, inclination $i = 72^{+5}_{-8}{}^{\circ}$ and mass ratio $q = 0.045^{+0.022}_{-0.016}$. Based

[1] It is called a spectroscopic period rather than an orbital period because it was derived from spectroscopy and a photometric period will be derived later through photometry for comparison.

[2] See section 3.1.2 of the original paper [11] for details, as they are beyond the scope of this work.

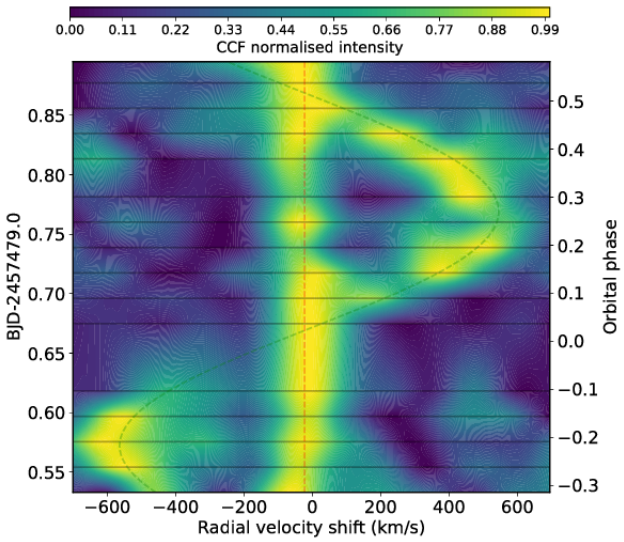

Figure 7. Trail of the CCFs for J1305 [11]. The colour map depicts the normalised intensity of the CCFs, the horizontal axis represents the radial velocity shift and the vertical axes show the orbital phase and a Barycentric Julian Date (BJD). The horizontal black lines mark the mid-exposure times of the group's observations. The dashed green line represents the best sinusoidal fit for the peaks, while the dashed red line represents the mean value for a secondary peak seen as a constant shift from the origin of the horizontal axis. This peak was identified as contamination from a nearby star. *Source: Figure 2, Dynamical confirmation of a stellar mass black hole in the transient X-ray dipping binary MAXI J1305-704, D. Mata Sánchez et al.,* Monthly Notices of the Royal Astronomical Society, *Volume 506, Issue 1, September 2021, Pages 581–594, https://doi.org/10.1093/mnras/stab1714.*

on the periods derived, the group employed the spectroscopic period as the orbital period of the binary $P_{\rm orb} = 0.394 \pm 0.004\,{\rm d}$, since it is consistent with the photometric period. The inclination and mass ratio are not well constrained, however.

With all the relevant parameters ready, the group started the mass determination by calculating the lower limit for the compact object mass with the mass function (3) by setting $M_c = 0$ and $i = 90°$, giving

$$f(M_X) = \frac{M_X \sin^3 i}{(1+q)^2} = \frac{K_c^3 P_{orb}}{2\pi G} = \frac{(554\,\mathrm{km/s})^3 \cdot (0.394 \cdot 86\,400)\,\mathrm{s}}{2\pi G}$$
$$= 6.9 \pm 0.3\, M_\odot.$$

This lower limit confirms that J1305 contains a black hole, because the object would be far too heavy to be a neutron star. However, in order to solve the system's dynamics, the inclination and mass ratio needed to be better constrained.

For the mass ratio, the group compared several potential values, eventually settling on a normal distribution of $q = 0.05 \pm 0.02$, truncated to $0.01 < q < 0.07$. This also constrains the companion mass as $0.35 \pm 0.12\, M_\odot$. For the inclination, after careful analysis, the group had to settle on favouring the previously derived inclination of $i = 72^{+5}_{-8}°$, as it is consistent with a previously established range of $60° < i < 82°$, which was based on X-ray dipping phenomenology.

With that, the masses could now be constrained with the mass functions (3) and (4). The resulting black hole mass is

$$M_X = \frac{6.9\, M_\odot}{\sin^3 i}(1+q)^2 = \frac{6.9\, M_\odot}{\sin^3(72°)}(1+0.05)^2 = 8.9^{+1.6}_{-1.0} M_\odot$$

and the companion mass is

$$M_c = \frac{0.35\, M_\odot}{\sin^3 i}(1+q)^2 = 0.43 \pm 0.16\, M_\odot.$$

2.2 Scaling methods

For an accreting object, like a black hole, something called X-ray variability can be observed over a range of frequencies. This means that at a given

state, the power of the X-ray emission coming from the object varies based on frequency. The amplitude of the variability is called excess variance. [12]

To preface the scaling methods, it is useful to understand what power density spectra (PDS) are. By extensively observing the spectra of X-ray binaries in different states, PDS have been constructed to measure the X-ray variability. PDS are visualised by plotting the product of frequency and power over a frequency range. Figure 8 contains six example PDS from [12]. This creates a spectrum that can be (roughly) approximated by a broken power law (often doubly-broken). The frequency where a break happens in the spectrum is known as a break frequency. It turns out that the high-frequency spectral shape after the last break (i.e. above the break frequency) remains very constant for a given source and scales with the object's mass [12].

Based on this and by assuming that the spectral shape of the high-frequency tail is universal, the shape of the PDS can be written as [12]

$$P_\nu = C_M \left(\frac{\nu}{\nu_0} \right)^{-2}, \tag{5}$$

where ν is frequency, ν_0 is an arbitrary frequency and C_M is a mass-dependent normalisation of the high-frequency tail at ν_0. The excess variance can then be calculated in a given frequency band between ν_1 and ν_2 above the break frequency either directly from a light curve or from the PDS as [12]

$$\sigma^2_{\text{nxs}} = \int_{\nu_1}^{\nu_2} P_\nu \mathrm{d}\nu = C_M \nu_0 \left(\frac{\nu_0}{\nu_1} - \frac{\nu_0}{\nu_2} \right). \tag{6}$$

For reliability, the chosen frequency band should be significantly above the break.

At the heart of scaling methods lies the question: "Are active galactic nuclei scaled up versions of galactic black hole binaries?" [12]. As a result, these methods are mainly used for AGNs, but can still be useful for some galactic objects. The idea is to estimate the object's mass based on other available properties by using relations. Several kinds of relations are used,

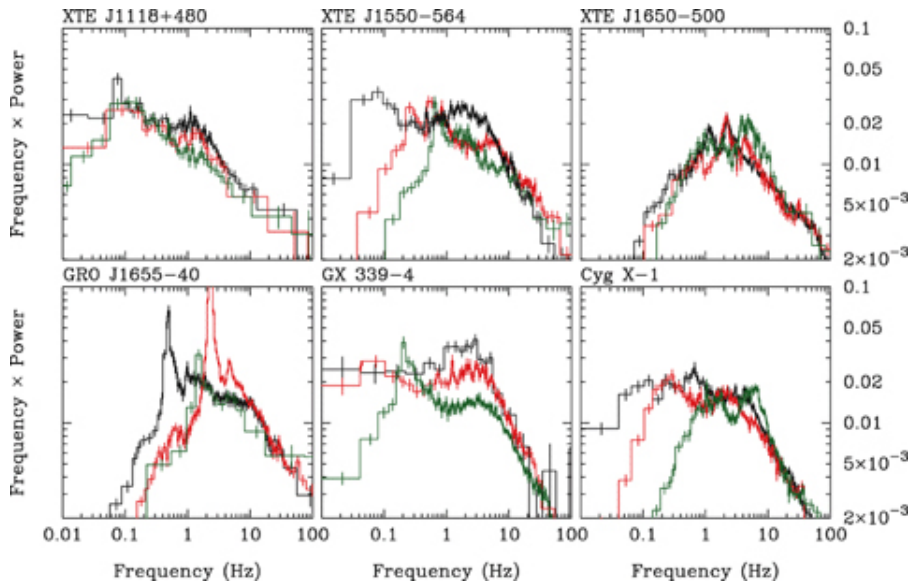

Figure 8. PDS of 6 black hole X-ray binaries. Each plot shows three spectra in different spectral states [12]. *Source: Figure 1, High-frequency X-ray variability as a mass estimator of stellar and supermassive black holes, M. Gierliński, M. Nikołajuk, B. Czerny,* Monthly Notices of the Royal Astronomical Society*, Volume 383, Issue 2, December 2007, Pages 741–749.*

especially for AGNs. For galactic objects, based on linear fits over the PDS of several galactic objects, Gierliński et al. [12] give the following

$$M_{\mathrm{X}} = \frac{C}{C_M} = \nu_0 \left(\frac{\nu_0}{\nu_1} - \frac{\nu_0}{\nu_2} \right) \frac{C}{\sigma^2_{\mathrm{nxs}}}, \tag{7}$$

where $C = 1.24\,\mathrm{M}_\odot\,\mathrm{Hz}^{-1}$ is a constant determined by comparing C_M to known BH masses, as shown in figure 9.

Furthermore, Czerny and Nikołajuk [5] highlight the following form of (7)

$$M_{\mathrm{X}} = 1.24 \frac{T - 2\Delta t}{\sigma^2_{\mathrm{nxs}}} M_\odot, \tag{8}$$

where T is the duration of a single X-ray lightcurve in seconds and Δt is its bin size, also in seconds. Note that in [5], the time bin Δt (as δt) is given

without its coefficient of 2, but based on the references, this is most likely an error. The constant at the beginning is also given as $1.92\,M_\odot\,s^{-1}$, but this is a simple matter of choice, as several slightly different values for C have been inferred from different sources [13]. In this case, $1.92\,M_\odot\,s^{-1}$ was chosen for consistency with broad line Seyfert 1 galaxies. The units used for C also vary between $M_\odot\,Hz^{-1}$ and $M_\odot\,s^{-1}$, the former being a result of Gierliński et al. dividing their constant C by ν_0^2 [12] (see also footnote 3 of [13, p. 2145]). This has no effect on the numerical value because [12] used $\nu_0 = 1\,Hz$.

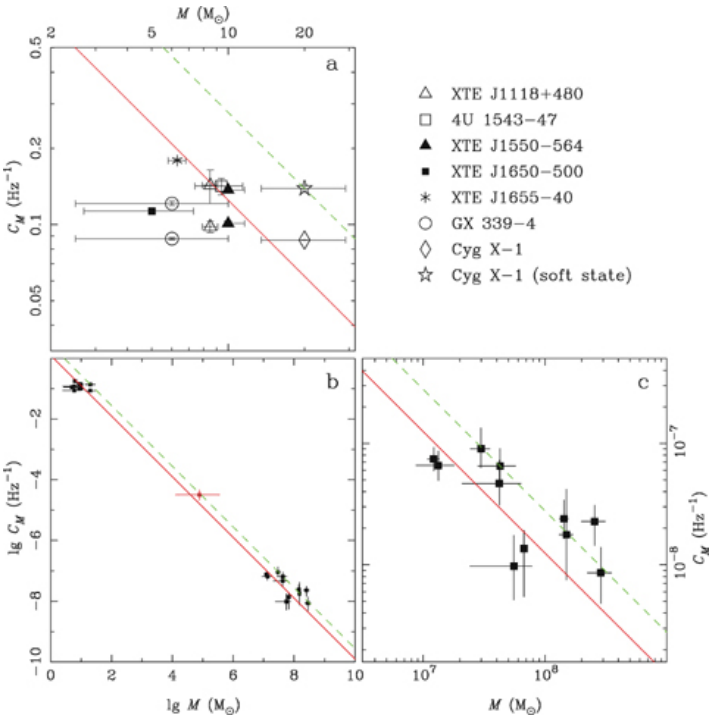

Figure 9. Fitting the constant C (red diagonal line) over the dependence of C_M on black hole mass [12]. Panel a shows X-ray binaries, c shows supermassive black holes from Seyfert 1 galaxies and b shows both as an overview. Note that this fit results in $C = 1.25\,\mathrm{M}_\odot\,\mathrm{Hz}^{-1}$, but $C = 1.24\,\mathrm{M}_\odot\,\mathrm{Hz}^{-1}$ is later specified for X-ray binaries only (see source for details). *Source: Figure 7, High-frequency X-ray variability as a mass estimator of stellar and supermassive black holes, M. Gierliński, M. Nikołajuk, B. Czerny,* Monthly Notices of the Royal Astronomical Society*, Volume 383, Issue 2, December 2007, Pages 741–749.*

2.3 Spectra fitting methods

If we can assume that we have a sufficiently reliable model of the emission coming from the compact source, we can utilise spectra fitting methods to get estimates for the object's mass. These methods rely on advanced models

that can be very situational and depend on the object having a fairly standard accretion disc. Such models depend on multiple factors, however, including mass, accretion rate, spin and even the viewing angle [5]. This means that in most cases with galactic sources, these methods prove more useful for inferring the spin, as the mass can at this point be estimated more reliably with the dynamical methods.

The core concept is to model out the accretion disc as accurately as possible (or practical) and apply that model to infer the object's properties. For a comprehensive example, see [14].

3 Caveats

In this section, some specific caveats, including advantages and disadvantages for specific types of sources are highlighted. These are just scratching the surface and references for further reading are provided. For a general overview, see e.g. [1].

3.1 Pulsars in high-mass X-ray binaries

Eclipsing pulsars in high-mass X-ray binaries allow for some of the best prospects for accurate mass determination, because the projected orbital velocities of both binary components can be measured thanks to the Doppler shift of the donor's photospheric lines combined with the neutron star pulse's timing delays [1]. Timing refers to how the timing of pulsars can provide very accurate values for the range of the pulsar relative to the system's centre of mass, which allows for very precise Keplerian parameters (i.e. its orbital properties). For details and a great review from the neutron star point of view, see [15].

However, the largest population of these pulsar binaries belong to a sub-

class of X-ray binaries known as Be/X-ray binaries. In these systems, the optical (non-compact) companion is a Be star, a non-supergiant fast-rotating B-type star with a luminosity class III–V, which has at some point shown spectral lines in emission. For specifics, see [16]. Generally, these systems have very wide and eccentric orbits, where the neutron star only periodically accretes material during periastron (the point of closest approach) passages or through episodic disc instability events [1]. The scarcity of eclipsing systems combined with the very long orbital periods makes mass determination in these systems extremely difficult to perform reliably.

3.2 Black holes in high-mass X-ray binaries

High-mass X-ray binaries are persistent X-ray sources, but their X-ray luminosity is low enough to not mask the optical companion and having negligible irradiation effects. Even the accretion disc's effects on the light curve can be ignored, meaning that the systematic effects described in section 2.1 do not affect it. Despite this, there are limitations, still. The mass of the companion and its uncertainty has a dramatic effect on the mass of the black hole. The companion stars in these systems tend to be less massive than their spectral type would imply due to mass transfer and even binary evolution. The mass transfer in high-mass X-ray binaries is not driven by Roche lobe overflow, due to the massive companion, but rather mostly by stellar winds. This means that the companion is not necessarily filling its Roche lobe, which is one of the assumptions made when using rotational broadening and ellipsoidal models. Using these models regardless would lead to underestimates in the mass ratio and inclination. Additionally, emission caused by the stellar winds can contaminate the measured radial velocities.

These challenges are overcome by including extra parameters to the models, like a Roche lobe filling factor. A prime example of how different con-

straints can be used would be measurements performed on Cygnus X-1. It has been a subject of deep observations throughout virtually all X-ray missions. See e.g. the latest Cyg X-1 mass determination by Miller-Jones et al. [17]. For more details on the case of black holes in high-mass X-ray binaries, see e.g. [8].

3.3 Short period low-mass X-ray binaries

Another case would be a low-mass X-ray binary with a period of a day or less, where the companion gets overwhelmed by the accretion luminosity, i.e. it cannot be directly detected. The masses can still be somewhat constrained by utilising the Bowen technique, where fluorescence lines excited on the X-ray heated face of the companion star are employed. This yields the companion's radial velocity semi-amplitude, but a so-called K-correction needs to be applied to get the true value. This is necessary because the Bowen lines' radial velocity curves are biased since they are drawn from the irradiated face of the star rather than the star's centre of mass. A typical example case of this is the X-ray binary Scorpius X-1 (where the Bowen lines were first detected), see e.g. [18]. See also section 4.1 of [8].

3.4 Ultraluminous X-ray sources

Eddington luminosity, also called the Eddington limit, is the maximum luminosity an object can achieve while hydrostatic equilibrium is maintained. Non-nuclear sources that – under the assumption of isotropic emission – show luminosities comparable to or above the Eddington luminosity of stellar black holes are called ultraluminous X-ray sources (ULXs). Explaining the cause for the high luminosity of these sources is an ongoing discussion. Suggested explanations include these systems hosting an intermediate-mass black hole, or different accretion mechanisms causing super-Eddington accretion rates.

For a review on ULXs, see e.g. [19]. ULXs are also discussed in section 5.2 of [8].

4 Closing thoughts

Having multiple approaches to determining the masses of compact objects greatly improves the reliability of such measurements, as any singular method can produce more or less volatile results. The systematic nature of the measurement errors further complicates our ability to accurately determine the exact error margins of a given measurement. Therefore, it is crucial to utilise as many different approaches as possible or practical and look for consistencies to draw conclusions on.

As previously highlighted, the dynamical methods stand as the most important and accurate method for stellar black holes and neutron stars. Despite the apparent specific conditions required for using these methods, the nature of the objects observed still allows for these to work in most cases.

It is also worth noting that gravitational wave studies play an important role in future mass measurements by providing mass ratios and new models. For an in-depth review, see [20].

Yet we still have questions to answer. Possibly the most prominent of these has to do with intermediate-mass black holes (IMBH) and their possible relation to ULXs. We are yet to confirm the existence of a single IMBH, but some ULXs are considered promising candidates [19].

Another important question is the mass gap problem. Gathering reliable data on the masses of different compact objects is crucial for the creation of a comprehensive mass distribution. This has implications not only for the formation of these compact objects, but also for our understanding of supernovae and binary physics [4].

References

[1] J. Casares, P. G. Jonker, and G. Israelian. “X-Ray Binaries”. In: *Handbook of Supernovae*. Ed. by A. W. Alsabti and P. Murdin. Cham: Springer International Publishing, 2017, pp. 1499–1526. ISBN: 978-3-319-21846-5. DOI: 10.1007/978-3-319-21846-5_111. URL: https://doi.org/10.1007/978-3-319-21846-5_111.

[2] S. E. Motta et al. “The INTEGRAL view on black hole X-ray binaries”. In: *New Astronomy Reviews* 93 (May 12, 2021), p. 101618. DOI: 10.1016/j.newar.2021.101618. arXiv: 2105.05547 [astro-ph.HE].

[3] J. M. Lattimer. “The Nuclear Equation of State and Neutron Star Masses”. In: *Annual Review of Nuclear and Particle Science* 62.1 (Nov. 2012), pp. 485–515. DOI: 10.1146/annurev-nucl-102711-095018. arXiv: 1305.3510 [nucl-th]. URL: https://ui.adsabs.harvard.edu/abs/2012ARNPS..62..485L.

[4] M. Fishbach, R. Essick, and D. E. Holz. “Does Matter Matter? Using the Mass Distribution to Distinguish Neutron Stars and Black Holes”. In: *The Astrophysical Journal* 899.1 (Aug. 2020), p. L8. DOI: 10.3847/2041-8213/aba7b6. arXiv: 2006.13178 [astro-ph.HE].

[5] B. Czerny and M. Nikołajuk. “Mass of black holes: The State of the Art”. In: *Memorie della Societa Astronomica Italiana* 81 (Oct. 2, 2009), p. 281. arXiv: 0910.0313 [astro-ph.HE].

[6] W. M. Farr et al. “The Mass Distribution of Stellar-Mass Black Holes”. In: *The Astrophysical Journal* 741.2 (Oct. 2011), p. 103. DOI: 10.1088/0004-637X/741/2/103. arXiv: 1011.1459 [astro-ph.GA].

[7] L. Kreidberg et al. “Mass Measurements of Black Holes in X-Ray Transients: Is There a Mass Gap?” In: *The Astrophysical Journal* 757.1

(Sept. 2012), p. 36. DOI: 10.1088/0004-637X/757/1/36. arXiv: 1205.1805 [astro-ph.HE].

[8] J. Casares and P. G. Jonker. "Mass Measurements of Stellar and Intermediate-Mass Black Holes". In: *Space Science Reviews* 183.1-4 (Dec. 2013), pp. 223–252. DOI: 10.1007/s11214-013-0030-6.

[9] M. G. Witte and G. J. Savonije. "Tidal evolution of eccentric orbits in massive binary systems". In: *Astronomy & Astrophysics* 366.3 (Feb. 2001), pp. 840–857. DOI: 10.1051/0004-6361:20000245.

[10] R. A. Wade and K. Horne. "The radial velocity curve and peculiar TiO distribution of the red secondary star in Z Chamaeleontis". In: *The Astrophysical Journal* 324 (Jan. 1988), p. 411. DOI: 10.1086/165905.

[11] D. Mata Sánchez et al. "Dynamical confirmation of a stellar mass black hole in the transient X-ray dipping binary MAXI J1305-704". In: *Monthly Notices of the Royal Astronomical Society* 506.1 (Sept. 2021), pp. 581–594. DOI: 10.1093/mnras/stab1714. arXiv: 2104.07042 [astro-ph.HE].

[12] M. Gierliński, M. Nikołajuk, and B. Czerny. "High-frequency X-ray variability as a mass estimator of stellar and supermassive black holes". In: *Monthly Notices of the Royal Astronomical Society* 383.2 (Dec. 2007), pp. 741–749. DOI: 10.1111/j.1365-2966.2007.12584.x. arXiv: 0710.1566 [astro-ph].

[13] M. Nikołajuk, B. Czerny, and P. Gurynowicz. "NLS1 galaxies and estimation of their central black hole masses from the X-ray excess variance method". In: *Monthly Notices of the Royal Astronomical Society* 394.4 (Apr. 2009), pp. 2141–2152. DOI: 10.1111/j.1365-2966.2009.14478.x. arXiv: 0901.1442 [astro-ph.GA].

[14] A. Sądowski et al. “Vertical dissipation profiles and the photosphere location in thin and slim accretion disks”. In: *Astronomy & Astrophysics* 502.1 (Feb. 2009), pp. 7–13. DOI: 10.1051/0004-6361/200911846. arXiv: 0902.2391 [astro-ph.HE].

[15] F. Özel and P. Freire. “Masses, Radii, and Equation of State of Neutron Stars”. In: *Annual Review of Astronomy and Astrophysics* 54.1 (Mar. 8, 2016), pp. 401–440. DOI: 10.1146/annurev-astro-081915-023322. arXiv: 1603.02698 [astro-ph.HE].

[16] P. Reig. “Be/X-ray binaries”. In: *Astrophysics and Space Science* 332.1 (Jan. 26, 2011), pp. 1–29. DOI: 10.1007/s10509-010-0575-8. arXiv: 1101.5036 [astro-ph.HE].

[17] J. C. A. Miller-Jones et al. “Cygnus X-1 contains a 21–solar mass black hole—Implications for massive star winds”. In: *Science* 371.6533 (Feb. 18, 2021), pp. 1046–1049. DOI: 10.1126/science.abb3363. arXiv: 2102.09091 [astro-ph.HE].

[18] L. Wang et al. “Precision Ephemerides for Gravitational-wave Searches – III. Revised system parameters of Sco X-1”. In: *Monthly Notices of the Royal Astronomical Society* 478.4 (June 4, 2018), pp. 5174–5183. DOI: 10.1093/mnras/sty1441. arXiv: 1806.01418 [astro-ph.HE].

[19] P. Kaaret, H. Feng, and T. P. Roberts. “Ultraluminous X-Ray Sources”. In: *Annual Review of Astronomy and Astrophysics* 55.1 (Aug. 2017), pp. 303–341. DOI: 10.1146/annurev-astro-091916-055259. arXiv: 1703.10728 [astro-ph.HE].

[20] L. Barack et al. “Black holes, gravitational waves and fundamental physics: a roadmap”. In: *Classical and Quantum Gravity* 36.14 (June 2019), p. 143001. DOI: 10.1088/1361-6382/ab0587. arXiv: 1806.05195 [gr-qc].